

CLINICAL SCIENCES

VOXEL-BASED INVESTIGATIONS OF REGIONAL CEREBRAL BLOOD FLOW ABNORMALITIES IN ALZHEIMER'S DISEASE USING A SINGLE-DETECTOR SPECT SYSTEM

Fabio L. S. Duran, Fernando G. Zampieri, Cassio C.M. Bottino, Carlos A. Buchpiguel, Geraldo F. Busatto

Duran FLS, Zampieri FG, Bottino CCM, Buchpiguel CA, Busatto GF. Voxel-based investigations of regional cerebral blood flow abnormalities in Alzheimer's disease using a single-detector SPECT system. Clinics. 2007;62(4):377-84.

PURPOSE: To evaluate the feasibility of using the *Statistical Parametric Mapping* (SPM) program for an automated, voxel-by-voxel assessment of regional cerebral blood flow (rCBF) deficits in Alzheimer's disease (AD) subjects relative to age-matched controls studied with a conventional, single-detector SPECT system.

METHODS: We used a databank of ^{99m}Tc -HMPAO images of 19 patients with a diagnosis of probable AD and 15 elderly healthy volunteers; data were acquired using an Orbiter-Siemens single-detector SPECT system. Using SPM, images were transformed spatially, smoothed (12mm), and the data were compared on a voxel-by-voxel basis with t-tests.

RESULTS: There were significant rCBF reductions in AD patients relative to controls involving regions predicted *a priori* to be affected in AD, namely the left temporal and parietal neocortices, and the right posterior cingulate gyrus ($p < 0.05$, corrected for multiple comparisons).

DISCUSSION: The location of rCBF reductions in AD subjects in our study is consistent with the deficits detected in previous functional imaging studies of AD using higher-resolution devices. This suggests the potential usefulness of using SPM for the analysis of data acquired with single-detector SPECT systems, despite the limited sensitivity and spatial resolution of such equipment.

KEY-WORDS: Statistical Parametric Mapping. Dementia. Functional Neuroimaging. Gamma-camera.

INTRODUCTION

Using the techniques of positron emission tomography (PET), single photon emission computed tomography (SPECT) and functional magnetic resonance imaging (MRI); it is now possible to acquire images of high anatomical resolution showing patterns of functional brain activity or neurotransmission *in vivo*.

Several studies using the above functional imaging techniques have compared groups of patients with Alzheimer's disease (AD) with healthy controls, most often measuring

resting regional cerebral blood flow (rCBF) or regional brain glucose metabolism.^{1,2,3,4} A pattern of hypoactivity in the temporal and parietal neocortices in association with AD has been the most characteristic finding in those studies, detected either by visual inspection or by conventional quantitative analyses using regions of interest (ROI).

Lately, automated methods have been developed for the analysis of functional imaging research data, allowing the comparison of rCBF values between different groups to be performed on a voxel-by-voxel basis. The most disseminated method for such purpose is the Statistical Parametric Mapping (SPM) program.⁵ Recent PET and SPECT studies using SPM-based image analysis methods have replicated the above findings of temporo-parietal neocortical hypoactivity in AD; moreover, these studies have been able to document

Institute of Psychiatry, São Paulo University Medical College Hospital
Email: gbusatto@terra.com.br
Received for publication on January 30, 2007
Accepted for publication on March 9, 2007

resting activity decrements also in the medial temporal region (where the neuropathological process that characterizes AD occurs first and with greatest severity), as well as in the posterior cingulate gyrus and precuneus.⁶ The involvement of the posterior cingulate gyrus and precuneus has been detected even in very early stages of AD,^{6,7,8} as well as in subjects at genetic risk for the disorder.⁹

SPECT studies of AD using the SPM approach have been invariably restricted to research centers that have access to sophisticated SPECT devices of two or more detectors, using imaging protocols of superior spatial resolution.^{10,11} Conventional, single-detector SPECT systems provide rCBF data of lower spatial resolution and sensitivity compared to multiple-detector systems, but are cheaper and more largely available, particularly in routine clinical services. However, it is not known whether single-detector SPECT systems can detect statistically significant rCBF deficits with the SPM approach in studies comparing AD samples to healthy controls. In the present study, we describe the application of the SPM methodology for the analysis of rCBF data acquired in our Institution with a conventional, single-detector SPECT system, in a group of AD patients compared to an age- and gender-matched healthy control group. Our goal was to evaluate the feasibility of using the SPM program for the analysis of rCBF data acquired with conventional SPECT devices, largely available in Brazil, attempting to replicate findings of regional hypoperfusion in AD patients reported in previous PET and SPECT imaging literature.^{6,11}

METHODS

Study sample

We used a dataset of rCBF SPECT images previously acquired from a group of 19 patients with probable AD (mean age = 74.63 years, SD=7.10, 7 males/12 females), recruited from the "Projeto Terceira Idade" (PROTER), Institute of Psychiatry, under the coordination of one of the authors (C.M.C.B.). Images were acquired following approval by the local ethics committee, and after subjects/relatives gave written informed consent; detailed explanations of the procedures involved were spelt out to each subject/relative.

The diagnosis of probable AD was made according to the criteria of the "National Institute of Neurological and Communicative Disorders/Stroke and Alzheimer's Disease and Related Disorders Association of the USA (NINCDS/ADRDA),¹² with basis on a semi-structured interview using the *Cambridge Mental Disorders of the Elderly Examination* (CAMDEX).¹³ Physical and neurological examina-

tion was also performed in all subjects, as well as blood screening, urine testing and computed tomography or structural MRI scanning, with the purpose of excluding other causes of dementia, as well as general medical conditions and neurological disorders that could affect brain structure and/or functioning. The severity of cognitive decline in AD patients was evaluated using the Mini-Mental State Examination (MMSE),¹⁴ with mean scores of 15.0 (DP= 8.9); this indicated a mean degree of dementia severity in the moderate range in the AD sample as a whole. The control group included rCBF SPECT images of 15 elderly healthy volunteers (mean = 71.60 years, SD= 3.85, 4 males/11 females). There were no significant differences between AD patients and controls either in regard to their mean age ($t=1.49$, $p=0.147$) or gender distribution ($p=0.72$). There were neither differences between AD patients and controls in regard to their mean number of years of education (mean = 6.21 years, SD= 4.06 and mean = 6.40 years, SD= 3.72 respectively, $t=-0.14$, $p=0.89$). All control subjects were interviewed through CAMDEX in order to exclude the presence of significant cognitive impairment and the presence of depressive symptoms. We also excluded from the control group any subjects with a history of current use of CNS-acting drugs. All subjects in the healthy control group had MMSE scores greater than 26.

SPECT image acquisition

Images were acquired after intravenous injection of 740MBq technetium-99m hexamethylpropylene-amine-oxime (^{99m}Tc-HMPAO) at rest (eyes closed and ears plugged). A single-detector SPECT system (Orbiter-Siemens) was used, equipped with low energy high-resolution (LEHR) collimators. A total of 128 projections was acquired on a 128x128 matrix (70,000 counts per projection). Images were reconstructed as 1-pixel (3.326mm) thick, transaxial slices, parallel to the orbitomeatal line, using the Filtered Back Projection method, after pre-filtering (Butterworth filter, cut-off frequency 0.35 cycles/pixel and order 7). We did not apply corrections for scatter and photon attenuation, given that we privileged the evaluation of cortical regions previously shown to be affected in the early stages of AD, rather than subcortical brain structures.

SPECT image processing

SPECT image analysis was performed using the SPM program,¹⁵ version 2002 (SPM2). Initially, this package spatially transforms the images, in order to make them compatible with an anatomical *template* that approximates the stereotaxic space of the Talairach and Tournoux atlas¹⁶. After

such spatial transformations, each voxel in all images will have the same coordinates in the x , y and z axes, corresponding approximately to the Talairach and Tournoux coordinates¹⁶. A customized SPECT template was created specifically for the present study, consisting of a mean image of all subjects. This strategy was aimed to match the template more closely to the population under investigation and the image acquisition protocols used.¹⁷ In order to build this template, the original SPECT images were spatially transformed to the standard SPM SPECT template, based on the Montreal Neurological Institute (MNI) template.¹⁸ Such a spatial normalization step was restricted to linear 12-parameter affine transformations, in order to minimize deformations of the original images. Subsequently, images were smoothed with an isotropic Gaussian kernel (12 mm FWHM), and averaged to provide the mean SPECT image in stereotactic MNI space.

The processing of the original images from all AD patients and controls was then carried out, beginning by spatial transformations of images to our study-specific SPECT template, with 12-parameter linear as well as nonlinear (3x4x3 basis functions) transformations. Spatially normalized images were then re-sliced using tri-linear interpolation to a final voxel size of 2x2x2 mm³, and smoothed using a 12-mm Gaussian kernel.

Statistical analysis using the SPM program

Voxel-based comparisons of regional tracer uptake values between AD patients and healthy controls were performed using unpaired t-tests. With the purpose of accounting for inter-individual differences in global cerebral blood flow, the regional ^{99m}Tc-HMPAO uptake was standardized to the mean global uptake using proportional scaling. The measure of total brain radioactive uptake was obtained automatically by the SPM program, given by the mean counts of all voxels included in the SPECT volume of each subject, after the spatial transformations described above.

In order to reduce the number of statistical comparisons, only voxels with signal intensities above 50% of the mean global value were entered in the group comparisons. Resulting statistics were transformed to Z-scores, thresholded at $Z=2.33$ (corresponding to the $p<0.01$, single-tail), and displayed as statistical parametric maps (SPMs) into standard space. Firstly, we inspected the resulting SPMs to search for the presence of voxel clusters of significantly reduced rCBF in the AD group in brain areas that usually present functional deficits early during the course of the illness, including: the medial temporal region, the lateral temporal and parietal neocortices, the medial parietal cortex (precuneus) and the posterior cingulate

gyrus.⁶ The voxels mapped to each of those brain regions were circumscribed using the small volume correction (SVC) tool available in the SPM package, whereby we applied predefined, spatially normalized volumes of interest on the SPMs, resulting in search volumes of: (a) 2,130 voxels for the medial temporal region (encompassing the hippocampus, parahippocampal gyrus and amygdala); (b) 6,237 voxels for the lateral temporal neocortex (including the superior, middle, inferior and transverse temporal gyri, and the insula); (c) 6,941 voxels for the lateral parietal neocortex (encompassing the superior parietal, inferior parietal, angular and supramarginal gyri.); (d) 4,942 voxels for the posterior cingulate gyrus; and (e) 3,528 voxels for the medial parietal cortex. Any rCBF differences within those areas were reported as significant only if surviving correction for multiple comparisons ($p<0.05$); such correction was calculated using the two methods that have been validated for SPM-based rCBF PET or SPECT studies,¹⁵ namely: (i) correction at the level of cluster of contiguous voxels, which is based on Gaussian random field theory; and (ii) the family-wise error (FWE) correction at the voxel level. Subsequently, we described the presence of rCBF abnormalities in other, unpredicted regions; findings in these additional areas would only be reported as significant if surviving correction for multiple comparisons over the whole brain (search volume of approximately 274,135 voxels). In every analysis, we converted MNI coordinates of voxels of maximal statistical significance to the Talairach and Tournoux system.^{16,19}

RESULTS

The statistical parametric map showing the foci of significant rCBF reductions in AD patients relative to controls, using the global normalization method, is shown in Figure 1. Using the SVC tool, we detected areas of significantly reduced activity in the following brain regions predicted *a priori* to be affected in AD: the left lateral temporo-parietal neocortices, and the right posterior cingulate gyrus ($p<0.05$, corrected multiple comparisons). Information on the level of statistical significance and extent of these foci is given in Table 1. There were other clusters of between-group difference located in additional brain regions where functional deficits had been predicted *a priori*, namely the left medial temporal region, the left posterior cingulate cortex and the left precuneus; however, these clusters did not retain statistical significance after correction for multiple comparisons (Table 1).

In the statistical map investigating significant rCBF increases in AD patients relative to healthy controls, there were two unexpected foci of significant hyperactivity, lo-

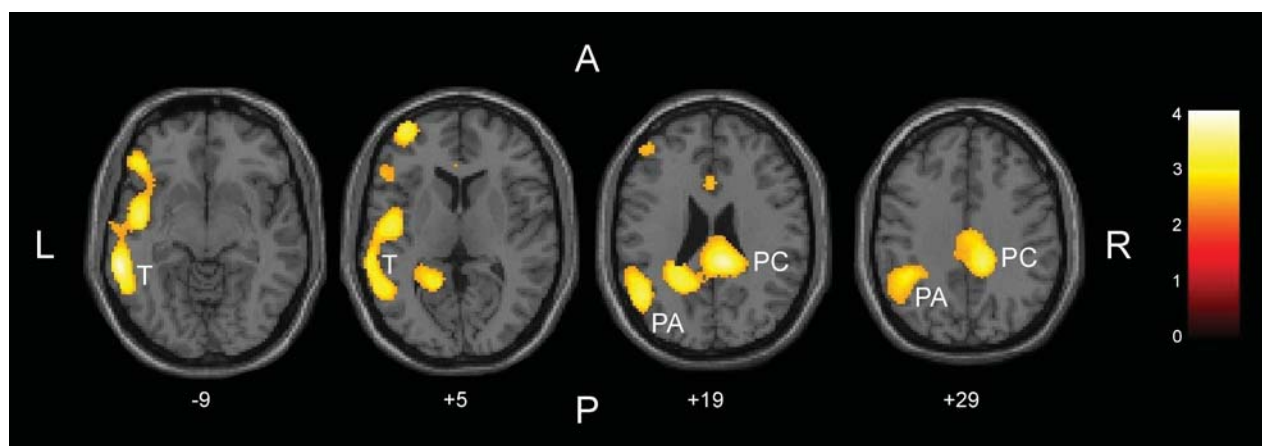


Figure 1 - Areas of significant regional cerebral blood flow (rCBF) reductions in patients with AD relative to healthy controls, using the global normalization method, are shown in yellow. Foci of significance were overlaid on transaxial brain slices of a structural MRI scan spatially transformed into an approximation to the Talairach and Tournoux stereotactic atlas.¹⁶ The numbers associated with each frame represent standard coordinates in the z axis. Statistical voxel values have been thresholded at $Z=2.33$ (corresponding to $p<0.01$, uncorrected for multiple comparisons). The brain regions where hypoactivity in the AD group had been hypothesized *a priori*, and which showed significant differences between the two groups (at the 0.05 level corrected for multiple comparisons) were: the left lateral temporal and parietal cortices (labeled respectively with the white-printed letters T and PA) and the posterior cingulate gyrus (PC). The coordinates of voxels of maximal statistical significance in each cluster, as well as their size, peak Z-scores and associated p values, are provided in Table 1. The figure also shows smaller foci or rCBF reductions in AD patients in the left inferior prefrontal cortex and anterior cingulate gyrus, but these findings did not retain significance after correction for multiple comparisons.

Table 1 – Areas of significantly reduced rCBF in subjects with AD (n=19) compared to healthy volunteers (n=15)

Regions + investigated	Side [§]	Coordinates [*]			Brain structure of maximal significant difference within each region (BA)	Peak [£] Z-Score	Number [#] of voxels	P value [§] (cluster level)	P value ^{§§} (voxel level)
		x	y	z					
Medial temporal lobe	Left	-18	-13	-22	Parahippocampal gyrus (BA 35)	2.47	51	NS	NS
Lateral temporal neocortex	Left	-43	-7	-4	Insula (BA 13)	3.31	882	0.04	NS
Lateral parietal neocortex	Left	-43	-60	18	Middle temporal gyrus (BA 39)	3.16	932	0.04	NS
Cingulate gyrus	Left	-11	-52	16	Posterior cingulate cortex (BA 30)	2.90	418	NS	NS
	Right	10	-40	24	Posterior cingulate cortex (BA 23)	3.63	617	0.04	0.01
Medial parietal cortex	Left	-13	-54	18	Precuneus (BA 31)	2.93	197	NS	NS

^{*} Brain regions where hypoactivity in the AD group was predicted *a priori*, circumscribed using the small volume correction (SVC) tool available in the SPM package.

[§] Brain hemisphere where group differences were identified.

^{*} Talairach and Tournoux¹⁶ coordinates of the voxel of maximal statistical significance within each area investigated.

[£] Z-score for the voxel of maximal statistical significance in each region.

[#] Total number of contiguous voxels in each region that surpassed the initial cutoff of $Z > 2.33$.

[§] Statistical significance after correction for multiple comparisons at the level of cluster of contiguous voxels (based on Gaussian random field theory).

^{§§} Statistical significance after family-wise error (FWE) correction for multiple comparisons at the voxel level.

Abbreviations: NS = non-significant; BA = Brodmann area.

cated respectively in: (i) the cerebellum bilaterally (4,541 voxels; maximal Z score = 3.84; coordinates_{x,y,z} of the voxel of maximal statistical significance = -13; -54; -22; $p < 0.003$ corrected for multiple comparisons at the cluster level); and (ii) the right pre- and post-central gyri (8,276 voxels; maximal Z score = 4.53; coordinates_{x,y,z} of the voxel of maximal statistical significance = 31; -15; 31; $p < 0.001$ corrected for multiple comparisons at the cluster level, and $p = 0.041$ at the voxel level).

DISCUSSION

In this study, we employed the automated SPM program to investigate, on a voxel-by-voxel basis, the presence of between-group rCBF differences using images acquired with a single-detector SPECT system. To the best of our knowledge, this is the first study in Brazil that applied voxel-based analysis methods to process SPECT data obtained using such a conventional and largely available gamma-camera system. Our comparison of images from a group of patients with AD relative to healthy controls led to the identification of rCBF abnormalities in areas that are broadly consistent with the regions where foci of hypofunction have been detected in previous PET and SPECT investigations of subjects with AD, namely the lateral temporo-parietal cortex and the posterior cingulate cortex.^{6,20} The relative consistency of our results with such previous functional imaging literature suggests the feasibility of applying the SPM program for the analysis of rCBF data of AD samples obtained using conventional, single-detector SPECT systems.

Although the findings above are encouraging, it should be mentioned that our sample included a proportion of AD patients with moderate or severe dementia. Therefore, one would have expected the presence of more extensive foci of cortical hypoactivity in our AD group relative to controls, involving the temporo-parietal cortex more largely and bilaterally, as well as affecting other regions, such as the medial temporal region, the precuneus, and the prefrontal cortex.^{6,11,21} This suggests that, due to the lower sensitivity of single-detector SPECT systems,²² the magnitude of rCBF deficits in a given sample may be underestimated when the SPM program is used to analyze data acquired with such a type of SPECT equipment. However, this possibility could not be directly ascertained in our study, as we did not obtain rCBF data from the same subjects using both our single-detector system and another, multiple-detector system affording greater sensitivity and spatial resolution.

Despite the limited sensitivity of single-detector SPECT scanners, our data suggest that the use of the SPM approach

for the statistical analysis of rCBF data acquired with those conventional systems may be useful, given the advantages of the SPM package over ROI-based methods. Among these advantages is the fact that SPM analyses are performed in a fully automated fashion, with no observer interference as in ROI-based or visual inspection methods. Moreover, SPM analyses are less cumbersome and more reproducible in comparison with the drawing of small ROIs over several sequential slices of the brain. Finally, the voxel-by-voxel inspection across the entire brain allows the detection of rCBF abnormalities in deep and medial structures that are difficult to assess reliably using ROI-based methods.

As in previous SPECT investigations of AD²³, our statistical parametric map investigating significant rCBF increases in AD patients relative to healthy controls (with covariance for the total counts in the brain) revealed areas of hyperactivity in the AD group. Such findings are interpreted as artifacts of the statistical analysis;²³ because the brain blood flow in AD patients is reduced in several gray matter areas, the proportional scaling of individual values to the total brain uptake leads to an overestimation of the relative rCBF measures in AD subjects in regions that are less affected by the disease process, such as the pre- and post-central gyri and cerebellar regions, all of which show as hyperactive in our AD subjects.

There are previous studies in which the SPM approach was used to perform statistical comparisons of functional imaging data from a single subject *versus* a control group of healthy volunteers, using either PET²⁴ or multiple-detector SPECT systems.^{25,26} This strategy has opened the possibility for using the SPM program in routine, single-case diagnostic applications in Neurology and Psychiatry.²⁴ Our preliminary results warrant further empirical evaluation as to whether the SPM program could be a useful clinical tool to aid in the assessment of single subjects imaged with one-detector SPECT systems, largely available in routine nuclear medicine services in Brazil. However, it is important to highlight that the manipulation of the SPM package demands basic knowledge about image processing methods and routines of the MATLAB program, and therefore should be used preferentially under the supervision of trained computer scientists. The need of such specialized staff may eventually prevent a more disseminated use of SPM in nuclear medicine services mainly dedicated to clinical work.

In conclusion, the results presented herein provide evidence that it is feasible to use the SPM program in rCBF studies comparing groups of AD patients and healthy subjects studied with conventional, single-detector SPECT systems. However, our findings were less robust in compari-

son to results reported in previous investigations of AD using more sophisticated SPECT systems, suggesting that the limited sensitivity of single-detector SPECT systems may underestimate findings of reduced rCBF, even when voxel-based programs such as SPM are used.

ACKNOWLEDGEMENTS

We thank Dr. Jaqueline Hatsuko Tamashiro for her assistance in the statistical analysis.

RESUMO

Duran Fabio LS, Zampieri FG, Bottino CCM, Buchpiguel CA, Busatto GF. Investigações voxel-a-voxel de anormalidades de fluxo sanguíneo cerebral regional na doença de Alzheimer usando equipamento de SPECT de detector único. Clinics. 2007;62(4):377-84.

OBJETIVO: Avaliar a viabilidade de emprego do programa Statistical Parametric Mapping (SPM) para investigar de forma automatizada, voxel-a-voxel, a presença de déficits de fluxo sanguíneo cerebral regional (FSCr) em pacientes com doença de Alzheimer (DA) comparados a sujeitos-controle pareados para idade, usando imagens de

SPECT adquiridas com um equipamento convencional de detector único.

MÉTODOS: Foi utilizado um banco de imagens adquiridas após injeção de ^{99m}Tc -HMPAO em 19 pacientes com diagnóstico provável de DA e 15 voluntários idosos saudáveis, usando um equipamento de SPECT Orbiter-Siemens de detector único. Empregando o programa SPM, as imagens foram transformadas espacialmente, suavizadas (12mm FWHM), e comparadas estatisticamente voxel-a-voxel entre os dois grupos, usando o teste de T.

RESULTADOS: Foram identificadas reduções significativas de FSCr nos pacientes com DA comparados aos con-

troles em regiões previstas *a priori* como afetadas por esta forma de demência, quais sejam os neocórtices temporal e parietal em hemisfério esquerdo e o cíngulo posterior direito ($p < 0,05$, corrigido para comparações múltiplas).

DISCUSSÃO: A localização dos focos de redução de FSCR em pacientes com DA no nosso estudo é, de forma geral, consistente com os achados de déficits cerebrais detectados em estudos anteriores de neuroimagem funcional na

DA realizados com equipamentos de resolução espacial mais alta. Isto sugere o potencial de utilidade do programa SPM para a análise de dados de SPECT adquiridos com equipamentos de detector único, apesar da sensibilidade e resolução espacial limitadas de tais aparelhos.

UNITERMOS: Statistical Parametric Mapping. Demência. Neuroimagem Funcional. Gama-câmera.

REFERENCES

- Gemmell HG, Sharp PF, Besson JA, Crawford JR, Ebmeier KP, Davidson J, Smith FW. Differential diagnosis in dementia using the cerebral blood flow agent ^{99m}Tc HM-PAO: a SPECT study. *J Comput Assist Tomogr.* 1987;11(3):398-402.
- Costa DC, Ell PJ, Burns A, Philpot M, Levy R. CBF tomograms with ^{99m}Tc -HM-PAO in patients with dementia (Alzheimer type and HIV) and Parkinson's disease—initial results. *J Cereb Blood Flow Metab.* 1988;8(6):S109-15.
- Rapoport SI, Horwitz B, Grady CL, Haxby JV, DeCarli C, Schapiro MB. Abnormal brain glucose metabolism in Alzheimer's disease, as measured by position emission tomography. *Adv Exp Med Biol.* 1991;291:231-48.
- Holman BL, Johnson KA, Gerada B, Carvalho PA, Satlin A. The Scintigraphic Appearance of Alzheimer's Disease: A Prospective Study Using Technetium- ^{99m}Tc -HMPAO SPECT. *The Journal of Nuclear Medicine.* 1992; 33(2):181-5.
- Friston KJ, Frith CD, Liddle PF, Frackowiak RS. Comparing functional (PET) images: the assessment of significant change. *J. Cereb. Blood Flow Metab.* 1991;11:690-9.
- Matsuda H. Cerebral blood flow and metabolic abnormalities in Alzheimer's disease. *Ann. Nucl. Med.* 2001;15:85-92.
- Ohnishi T, Hoshi H, Nagamachi S, Jinnouchi S, Flores LG, II, Futami S, Watanabe K. High-Resolution SPECT to Assess Hippocampal Perfusion in Neuropsychiatric Diseases. *The Journal of Nuclear Medicine.* 1995; 36(7):1163-9.
- Kogure D, Matsuda H, Ohnishi T, Asada T, Uno M, Kunihiro T, Nakano S, Takasaki M. Longitudinal Evaluation of Early Alzheimer's Disease Using Brain Perfusion SPECT. *The Journal of Nuclear Medicine.* 2000; 41(7):1155-62.
- Reiman EM, Chen K, Alexander GE, Caselli RJ, Bandy D, Osborne D, Saunders AM, Hardy J. Correlations between apolipoprotein E epsilon4 gene dose and brain-imaging measurements of regional hypometabolism. *Proc Natl Acad Sci U S A.* 2005;102(23):8299-302
- Szobot C, Roman T, Cunha R, Acton P, Hutz M, Rohde LA. Brain perfusion and dopaminergic genes in boys with attention-deficit/hyperactivity disorder. *Am J Med Genet B Neuropsychiatr Genet.* 2005;132(1):53-8.
- Colloby SJ, Fenwick JD, Williams ED, Paling SM, Lobotesis K, Ballard C, et al. A comparison of ^{99m}Tc -HMPAO SPET changes in dementia with Lewy bodies and Alzheimer's disease using statistical parametric mapping. *Eur J Nucl Med Mol Imaging.* 2002;29(5):615-22.
- Mckhann G, Drachman D, Folstein M, Katzman R, Price D, Stadlan EM. Clinical diagnosis of Alzheimer's disease: report of the NINCDS-ADRDA Work Group under the auspices of the Department of Health and Human Services Task Force on Alzheimer's Disease. *Neurology.* 1984;34:939-44.
- Roth M, Tym E, Mountjoy CQ, Huppert FA, Hendrie H, Verma S, et al. CAMDEX - a standardized instrument for the diagnosis of mental disorder in the elderly with special reference to the early detection of dementia. *Br. J. Psychiatry.* 1986;149:698-709.

14. Folstein MF, Folstein SE, McHugh PR. "Mini-mental state". A practical method for grading the cognitive state of patients for the clinician. *J. Psychiat. Res.* 1975;12:189-98.
15. Friston KJ, Holmes A, Poline JB, Price CJ, Frith CD. Detecting activations in PET and fMRI: levels of inference and power. *Neuroimage.* 1996;4:223-35.
16. Talairach J, Tournoux P. *A Co-planar Stereotaxic Atlas of Human Brain.* Stuttgart. Thieme; 1988.
17. Gispert JD, Pascau J, Reig S, Martinez-Lazaro R, Molina V, Garcia-Barreno P, et al. Influence of the normalization template on the outcome of statistical parametric mapping of PET scans. *Neuroimage.* 2003;19:601-12.
18. Mazziotta JC. Mapping human brain activity in vivo. *Western Journal of Medicine.* 1994;161:273-8.
19. Brett M, Johnsrude IS, Owen AM. The problem of functional localization in the human brain. *Nat Rev Neurosci.* 2002;3(3):243-9.
20. Chetelat G, Desgranges B, Eustache F. Brain profile of hypometabolism in early Alzheimer's disease: relationships with cognitive deficits and atrophy. *Rev Neurol (Paris).* 2006;162(10):945-51.
21. Encinas M, De Juan R, Marcos A, Gil P, Barabash A, Fernandez C, et al. Regional cerebral blood flow assessed with 99mTc-ECD SPET as a marker of progression of mild cognitive impairment to Alzheimer's disease. *Eur J Nucl Med Mol Imaging.* 2003;30(11):1473-80.
22. Tatsch K, Asenbaum S, Bartenstein P, Catafau A, Halldin C, Pilowsky LS, et al. European Association of Nuclear Medicine. European Association of Nuclear Medicine procedure guidelines for brain perfusion SPET using (99m)Tc-labelled radiopharmaceuticals. *Eur J Nucl Med Mol Imaging.* 2002;29(10):BP36-42.
23. Soonawala D, Amin T, Ebmeier Kp, Steele Jd, Dougall Nj, Best J, et al. Statistical parametric mapping of (99m)Tc-HMPAO-SPECT images for the diagnosis of Alzheimer's disease: normalizing to cerebellar tracer uptake. *Neuroimage.* 2002;17(3):1193-202.
24. Signorini M, Paulesu E, Friston K, Perani D, Colleluori A, Lucignani G, et al. Rapid assessment of regional cerebral metabolic abnormalities in single subjects with quantitative and nonquantitative [18F]FDG PET: A clinical validation of statistical parametric mapping. *Neuroimage.* 1999;9(1):63-80.
25. Barnes A, Lusman D, Patterson J, Brown D, Wyper D. The use of statistical parametric mapping (SPM96) as a decision aid in the differential diagnosis of dementia using 99mTc-HMPAO SPECT. *Behav Neurol.* 2000;12(1-2):77-86.
26. Rocha ET, Alves TCTF, Garrido GEJ, Buchpiguel CA, Nitrini R, Busatto Filho G. Novas técnicas de neuroimagem em psiquiatria: qual o potencial de aplicações na prática clínica? *Revista Brasileira de Psiquiatria.* 2001;21(supl 1):58-60.